

# Magnetic Shielding Implementation in the Small Satellite Reaction Wheel

Satriya UTAMA\*<sup>1</sup>, Deddy El AMIN<sup>1</sup>, M. Arif SAIFUDIN<sup>1</sup>, Moh. Farid HUZAIN<sup>1</sup>,  
Widya ROZA<sup>1</sup>, Chusnul Tri JUDIANTO<sup>1</sup>, Mohammad MUKHAYADI<sup>1</sup>

\*Corresponding author

<sup>1</sup>Research Center for Satellite Technology,  
National Research and Innovation Agency,  
Jl Cagak Satelit No.08 KM 0.4, Bogor 16310, Indonesia,  
satriya.utama@brin.go.id\*

DOI: 10.13111/2066-8201.2024.16.1.11

Received: 08 November 2023/ Accepted: 10 January 2024/ Published: March 2024

Copyright © 2024. Published by INCAS. This is an “open access” article under the CC BY-NC-ND license (<http://creativecommons.org/licenses/by-nc-nd/4.0/>)

**Abstract:** *Low Earth orbit satellites face challenges from Earth's magnetic field, causing attitude disturbances. Attaining a magnetic-dipole-free satellite is crucial. Layout optimization and in-orbit dipole compensation are common methods, but layout optimization can be impractical. In contrast, in-orbit dipole compensation struggles with rapidly changing magnetic dipoles like those from reaction wheel motors. This research proposes an alternative solution using Mu-metal, known for shielding against magnetic exposure. This shield can be applied to trap the magnetic field generated by the motors. Ground tests evaluated this approach. First, it determined the minimum distance between the magnetometer and the shield for accurate measurements with minimal interference, with the result of 10 cm as the least affected distance, particularly important for small satellite layout design. Second, it assessed the shield's effectiveness in trapping the motor-generated magnetic field. Tests showed a significant reduction in magnetic field magnitude and up to a 95% reduction in field fluctuations when the motor is activated. This research offers a practical solution for small satellite layout design, addressing the challenges posed by their compact dimensions. Mu-metal shielding proves effective for mitigating rapidly changing magnetic dipoles and enhancing magnetic cleanliness in low Earth orbit.*

**Key Words:** *Mu-Metal, reaction wheel motor, magnetic field, attitude disturbance, low earth orbit, magnetic cleanliness*

## 1. INTRODUCTION

BRIN (formerly LAPAN of Indonesia) has launched three small satellites into orbit, LAPAN-TUBSAT [1], LAPAN-A2 [2], and LAPAN-A3 [3]. All of them are low earth orbit (LEO) satellites. The satellite implements momentum bias attitude control by using the reaction wheels and magnetorquer as actuators in LAPAN-TUBSAT [4], LAPAN-A2 [5], and LAPAN-A3 [6]. As LEO satellites, the attitude control system has to deal with a major disturbance from atmospheric drag, gravity gradient, and the Earth's magnetic field. Among them, the Earth's magnetic field can become the biggest source of disturbance torque if the spacecraft has a magnetic dipole. There are various sources of magnetic dipole in the spacecraft, such as the reaction wheel motor, battery, magnetorquer, and wiring [7]. Eq. (1) shows torque resulting from an interaction between the Earth's magnetic field and satellite dipole,

$$\tau = mxB \quad (1)$$

where  $\tau$  is the magnetic torque vector,  $m$  is the satellite dipole and  $B$  is the Earth's magnetic field vector.

The torque generated from the Earth's magnetic field can be useful for attitude control as shown in [4], [8], [9]. However, the existence of satellite dipole is much of a problem if not handled properly. Some studies to minimize satellite dipole have already been done. Most of them are satellite layout optimization to achieve magnetic cleanliness [10], [11]. This method can give satisfying results but is not always easy to apply for any satellite. Besides magnetic cleanliness, other constraints such as mass distribution and wiring can complicate the problem, especially in small satellites where the space is very limited. Other studies show methods such as in-orbit magnetic dipole compensation [12], [13]. This method needs to estimate the spacecraft dipole first [14], [15] and then compensate for the dipole using a magnetic coil [12]. To compensate for the dipole, the magnetic coil should be continuously active and requires satellite power.

The dipole can be a constant or variable [15]. If the dipoles are constant, simple compensation can be introduced [14]. When the dipole varies, the compensation needs to be adjusted for each dipole change. Therefore, this method is difficult to implement on a rapidly changing magnetic dipole without an active control [16].

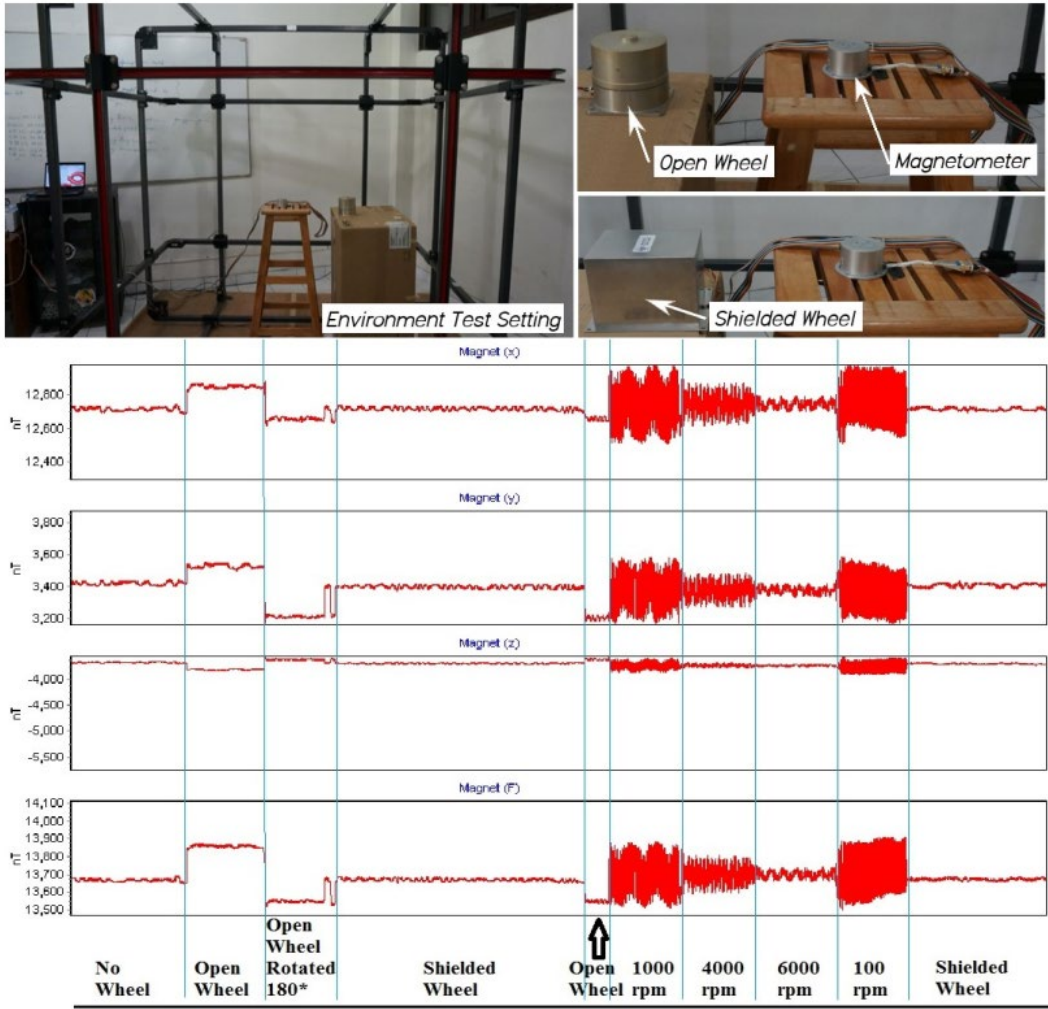
One of the spacecraft devices that makes the magnetic dipole change rapidly is the reaction wheel motor. The dipole value depends on the relative position between the rotor and the motor stator [17]. As the wheel rotor stops, the direction of the magnetic dipole depends on the actual end position of the wheel rotor.

Therefore, the dipole compensation depends on whether the wheel rotors are rotating or not, since it will need adjustment just after changing the operating status of the wheels from active to idle or vice versa. Magnetic shielding could probably be a more suitable and simpler alternative for dealing with magnetic dipole in this case. Magnetic shielding works by redirecting the magnetic field, it doesn't block the path. Magnetic shielding can be provided by special materials such as Mu-metal, a very high permeability of nickel-iron soft ferromagnetic alloy, which is commonly used to protect sensitive electronic equipment against static or low-frequency magnetic fields.

While the satellite applies the momentum bias method, so only one wheel works continuously to conserve the momentum, the remaining wheels work intermittently to reduce nutation. Once the wheel has finished damping the nutation, it will stop at any position so that the dipole of the spacecraft will change at any time.

This phenomenon, which has been observed since the first BRIN satellite, LAPAN-TUBSAT, has made satellite attitude control more complicated [18]. Hence, on the LAPAN-A2 and LAPAN-A3 satellites, all wheels are covered with Mu-metal shields [7]. Fig. 1 shows the test set-up and results on the LAPAN-A3 where the whole wheel unit is shielded by a Mu-metal.

The implementation of the Mu-metal shield has been reported to be quite effective on both satellite missions, but it costs a significant additional weight due to the high density of Mu-metal. In the LAPAN-A3 satellite, the utilization of the Mu-metal shield almost doubled the mass of the system with a 1.46 kg Mu-metal used for shielding a 1.52 kg wheel unit. Therefore, in the next BRIN satellite mission, the implementation of the Mu-metal shield will only be applied to the motor wheel section as shown in Fig. 2. Fig. 3 shows the size comparison of the Mu-metal shield in the LAPAN-A3, the wheel unit of the satellite, and the new Mu-metal shield for the motor wheel that will be used for the next satellites.



\* Wheel position is rotated 180 degree on its axis

Fig. 1 Reaction Wheel Shielding on LAPAN-A3: ground test set-up and results [7]

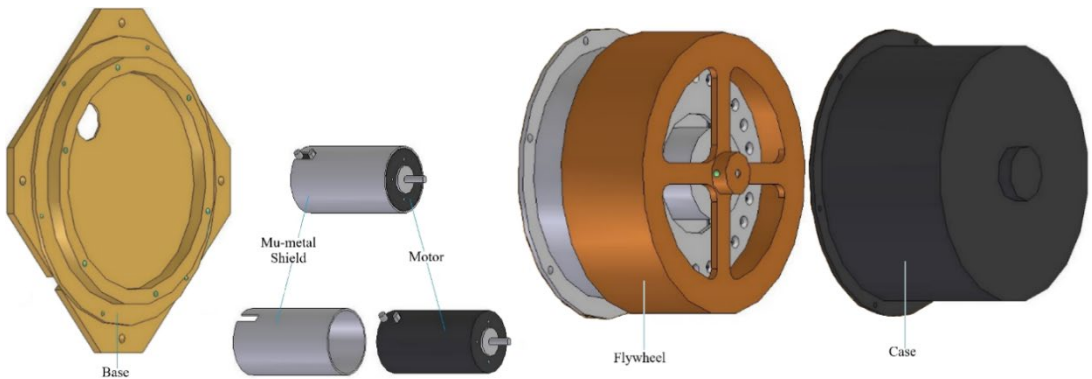


Fig. 2 Mu-metal shield on the wheel motor

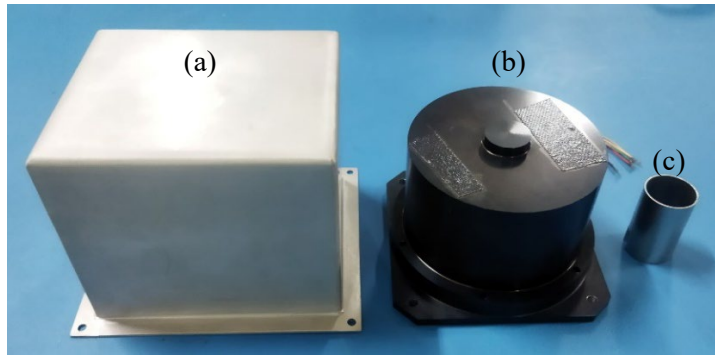


Fig. 3 Comparison of (a) the Mu-metal shield used in LAPAN-A3, (b) the wheel unit of LAPAN-A3, and (c) the Mu-metal for the next satellite

While the previous satellites used four identical wheels each, the next BRIN satellite will use two types of reaction wheels which have different momentum storage capacities. That's why it needs to use different types of motors, namely small motor and big motor, as shown in Table 1. Accordingly, two magnetic shielding tubes with 1 mm thick Mu-metal material were designed.

Table 1 - Specifications of the reaction wheel motors in the BRIN satellites

	Small Motor	Big Motor	Unit
Type	Faulhaber S2444 048 B	Faulhaber S3564 048 B	
Nominal Voltage	48	48	V
Diameter	24	35	Mm
Height	44	64	Mm
Mass	98	311	G
Housing material	aluminum, black anodized	aluminum, black anodized	
Magnet material	SmCo	SmCo	

In this study, a ground test setup was conducted through magnetometer measurements to perceive the effect of the Mu-metal shield on the magnetic dipole generated by the reaction wheel motor. Since the Mu-metal shield can affect the measurement by redirecting the magnetic field around, the placement of the magnetometer against the Mu-metal shield has to be considered carefully. Knowing the minimum distance between the magnetometer and the Mu-metal shield will also be very useful for satellite missions carrying a scientific magnetometer as one of the payloads to measure the Earth's magnetic field [19]. This study is also critical for the layout of spacecraft subsystems to mitigate magnetic incompatibility when the reaction wheel is in close proximity to any magnetically sensitive instruments [20].

A similar study was carried out on the Europe Clipper satellite to implement a Mu-metal shield on the wheel motor, with the expectation of reducing the static magnetization [20]. Since the Europa Clipper that will be flown to study Jupiter's moon is a large satellite with a launch mass of 6065 kg and dimensions of 6 m height with a solar panel span of 22 m, it uses a 1 m distance as the basis of the measurement of the wheel's magnetic field. This distance is achievable for a big satellite such as Europe Clipper but difficult to implement on smaller and less complex satellites. Hence, our study will search for more suitable distances that are more realistic to be implemented on small satellites. This distance can be used as the basis of the magnetic measurements and also a recommendation for small spacecraft subsystem layouts to minimize magnetic interference. Once the least affected distance is found, it will be used as

the basis for the experiment to see the effectiveness of the Mu-metal shielding on the wheel motors. Moreover, our research also investigates the ability of the Mu-metal shield to not only mitigate static magnetization but also shield against varying magnetic sources. While the Europa Clipper mission uses multi-layer Mu-metal shielding to eliminate wheel-generated magnetic fields, small satellites require a much simpler design. The design that requires more space is not suitable for small satellites which have compact and tiny space characteristics. Therefore, a simple design of shielding tubes with 1 mm thick of Mu-metal is introduced and investigated in this study.

## 2. METHODOLOGY

To carry out a ground measurement of the magnetic dipole generated by the reaction wheel motor, the first step is to find the less affected distance between the magnetometer and the magnetic shield. The measurement setting is depicted in Fig. 4 where the magnetometer is placed some distance from the Mu-metal. The distance ( $d$ ) is defined as the separation between the edge of the magnetometer and the edge of the Mu-Metal shield or motor which generates a magnetic dipole. The measuring distances were varied from 0 cm, 5 cm, and 10 cm and were compared to conditions where there was no Mu-metal shield or motor around the magnetometer. Each measurement will be carried out for at least 10 seconds to determine the stability of the measurement readings.

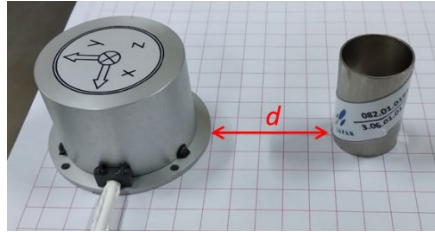


Fig. 4 Measurement setup that shows the distance ( $d$ ) between the magnetometer (left) and the Mu-metal shield (right), while the frame of reference ( $X, Y, Z$ ) is shown on the top of the magnetometer

Once the less affected distance is found in the previous step, the magnetometer will carry out the magnetic dipole measurement of the reaction wheel motor with or without the Mu-metal shield as displayed in Fig. 5 to determine the effectiveness of the shielding. The motor will be activated until it reaches a steady state speed at various motor current setups. As soon as the steady state condition is achieved, the magnetometer will start the measurement reading for at least 10 seconds.



Fig. 5 Magnetic field measurements of unshielded motor (above) and shielded motor (bottom)

### 3. RESULTS AND DISCUSSIONS

While the measurements are carried out in a laboratory that is not magnetically free, it is necessary to measure the environmental magnetic field conditions as a reference before engaging the Mu-metal shield or motor wheels. Fig. 6 shows a comparison between the reference condition and the magnetic field measured by a magnetometer at a distance of 0 cm, 5 cm, and 10 cm from the Mu-metal shield. Since magnetic fields are accumulative in nature, the influence of an object can be easily recognized through changes in the magnetic field compared to the initial conditions before the object's presence. Therefore, the effect of the Mu-metal shield on measurements by the magnetometer can be expressed as a difference in the magnetic field ( $\Delta B$ ) through the eq. (2), where  $\overline{B}_{ref}$  is the magnetic field reference obtained from the laboratory environment measurements.

$$\Delta B = \overline{B} - \overline{B}_{ref} \tag{2}$$

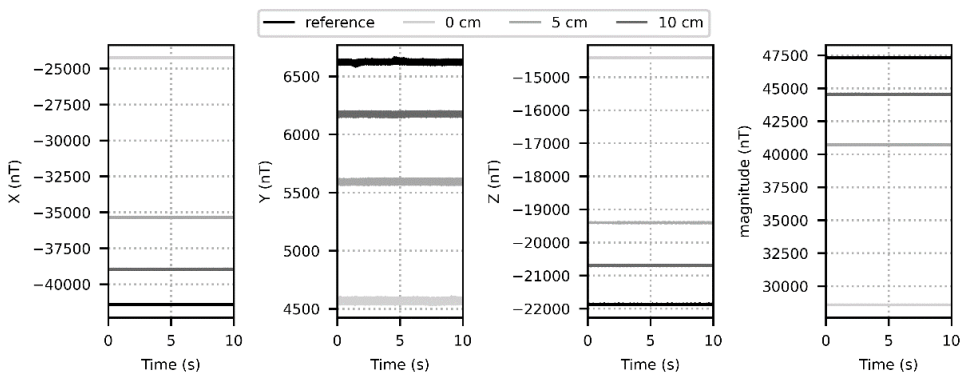


Fig. 6 Magnetic field measurements at a distance of 0 cm, 5 cm, and 10 cm from the small Mu-metal shield compared to the reference

Fig. 7 shows magnetic field readings of three different measurement distances for both big and small Mu-metal shields. The farther the measurement distance, the influence of the Mu-metal shield on the magnetic field will decrease significantly. At a distance of 10 cm from the Mu-metal shield, most of the measured magnetic field effect was below 3000 nT on the big shield and less than 1000 nT on the small one, so it was considered sufficient to observe the dynamics of the magnetic field generated by the wheel motors.

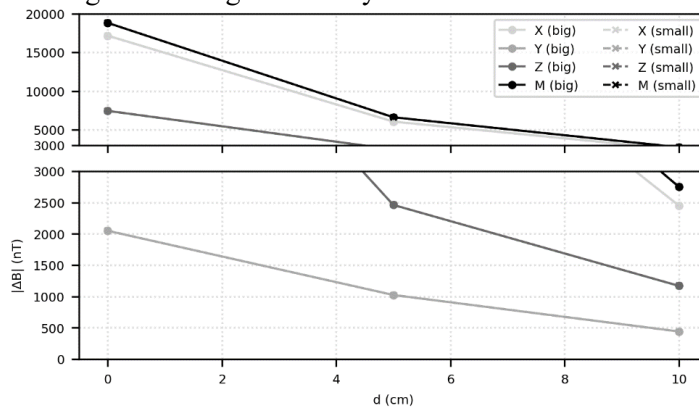


Fig. 7 Magnetic field difference as a function of the distance between magnetometer and Mu-metal for both small (solid line) and big (dashed line) Mu-metal

Since a distance of 10 cm from the Mu-metal shield is considered to have little effect on the magnetometer reading, all subsequent magnetic field measurements were carried out using that setting.

There are four measurement setups arranged to determine the effectiveness of the Mu-metal shield in dampening the residual magnetic dipole from the wheel motors, namely small unshielded motor, small shielded motor, big unshielded motor, and big shielded motor where each motor runs at four current variations of 0 mA (motor off), 60 mA, 90 mA, and 110 mA.

Table 2 shows the measurement results representing the mean and range of the magnetic field for each setup condition, where the range is defined as the measurement from the minimum peak value to the maximum peak value.

Meanwhile, the measurement of the environmental magnetic field is used as a reference which has a range of 80 nT, 55 nT, and 53 nT in the *X*, *Y*, and *Z* directions respectively, and 76 nT in magnitude, so it can be said that the measurement has a noise level of 80 nT.

The effectiveness of the Mu-metal shield can be easily determined by comparing the  $\Delta$  magnitude of the magnetic field between the shielded and unshielded motor when it is OFF. In this study, the shielding application has reduced the magnetic field magnitude from 3085 nT to 589 nT on the small motor, while on the larger motor, the magnetic field magnitude decreased from 3417 nT to 1910 nT.

Therefore, it can be said that the magnetic shielding application in this case is able to reduce 81% of the residual magnetic dipole on the small motor and 44% on the big motor.

Furthermore, in addition to its capability to reduce the magnitude of the magnetic field, the Mu-metal shield has demonstrated its ability to dampen magnetic field oscillations caused by rotating motors.

Once the motor is activated, the current will make the motor rotate, producing magnetic field oscillations with a certain amplitude and frequency.

In the unshielded motor configuration, this magnetic field oscillation pattern is clearly observed. A larger current will produce a larger frequency but not necessarily a larger amplitude.

However, sometimes those amplitudes and frequencies are not easy to observe, especially if the motor rotation speed causes oscillation that exceeds the sampling rate of the magnetometer which is 128 Hz.

Fig. 8 and Fig. 9 plot the dynamics of the magnetic field in the environment due to various motor activation settings for about 1 second of measurement reading. It appears that the magnetic field in the *Z* direction is not affected by the motor even though it is left open without shielding since it is parallel to the rotation axis of the motor.

Meanwhile, the magnetic field in the *X* and *Y* directions is most influenced by the activation of the motor wheel, which is normal since the motor will generate a magnetic dipole in those directions as shown in the measurement setup of Fig. 3.

The rotation of the motor will cause magnetic field oscillations with a range of up to 7645 nT in these directions.

While these large oscillations are not easily handled with a magnetic coil compensation scheme, they can be overcome simply by a Mu-metal shielding so that the oscillations are significantly reduced to less than 420 nT. This means that 95% of the magnetic field oscillation range can be suppressed.

Table 2 - Mean and range of the magnetic field under the influence of the reaction wheel motors for 10 seconds measurement reading

Measurement Setup		Mean	Range	Mean	Range	Mean	Range	Mean	Range
Reference		Bx		By		Bz		B Magnitude	
		-41416	80	6623	55	-21875	53	47304	76
		$\Delta B_x$		$\Delta B_y$		$\Delta B_z$		$\Delta$ Magnitude	
Small unshielded motor	Off	-2381	58	-1918	64	415	52	3085	77
	60 mA	-280	4276	-180	7645	389	720	2847	2230
	90 mA	-249	500	-334	639	480	292	668	494
	110 mA	-255	915	-357	1034	493	546	772	834
Small shielded motor	Off	-243	55	-234	60	483	55	589	81
	60 mA	-254	204	-411	420	459	110	677	267
	90 mA	-325	187	-189	356	336	170	509	263
	110 mA	-200	92	-266	111	663	92	743	111
Big unshielded motor	Off	-351	79	3000	75	1599	71	3417	64
	60 mA	-45	4120	-1353	6643	1590	572	3128	3194
	90 mA	-42	1300	-1351	2036	1591	557	2189	1623
	110 mA	88	1261	-1185	2014	1750	557	2221	1489
Big shielded motor	Off	124	64	-1116	69	1544	72	1910	73
	60 mA	146	227	-1129	431	1795	92	2129	212
	90 mA	67	179	-908	251	1662	152	1895	218
	110 mA	37	107	-987	170	1445	161	1751	201

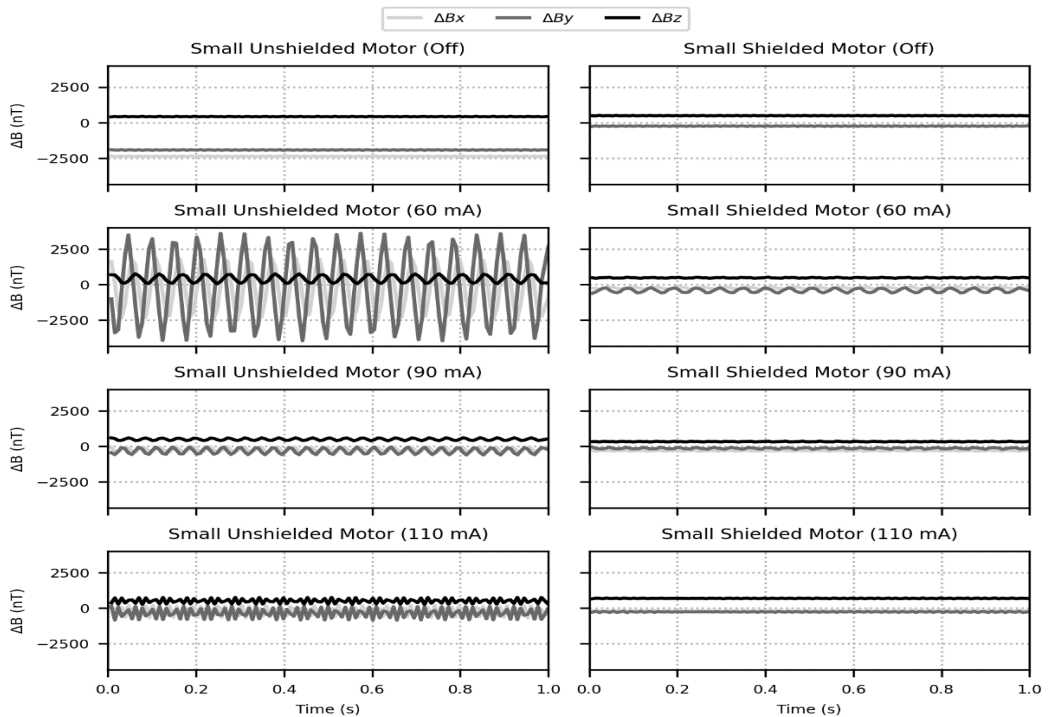


Fig. 8 Magnetic field differences under the influence of the small motor: unshielded (left) and shielded (right)

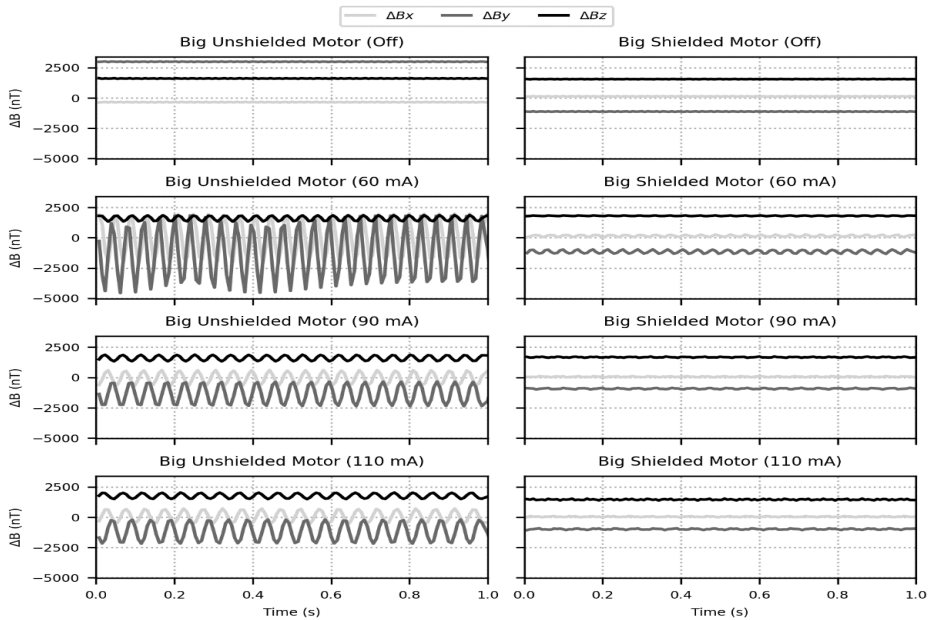


Fig. 9 Magnetic field differences under the influence of the big motor: unshielded (left) and shielded (right)

#### 4. CONCLUSIONS

In this study, we have explored the effectiveness of Mu-metal shields in mitigating the magnetic interference caused by the rapid changes in magnetic dipoles, particularly in the context of the reaction wheel motor within small spacecraft. Mu-metal shields have shown promise in addressing this issue, yet their high density adds significant weight to the spacecraft, prompting the need for efficient application to minimize weight costs. Our ground-based measurements have provided valuable insights into the impact of Mu-metal shields on the magnetic dipoles generated by the wheel motor. Our experiments have yielded encouraging results, demonstrating the ability of a simple design of a 1 mm thickness shielding tubes of Mu-metal to reduce the residual magnetic dipole by up to 81% and decrease the range of magnetic field fluctuations by up to 95%. This substantiates the effectiveness of Mu-metal as a magnetic shield for reaction wheel motors in spacecraft. On the other side, to optimize the application of Mu-metal shielding for a spacecraft using a magnetometer, the magnetometers should be positioned at a minimum distance of 10 cm from the Mu-metal or motor to obtain less affected results. A distance that is realistically easy to implement on any small satellite.

As a basic research that presents the effectiveness of Mu-metal shields with a simple one-layer design, it could be followed up with more complex shielding designs that are lighter and more effective so that they are more interesting to investigate. Likewise, other alternative materials that are lighter need to be tried and compared with current achievements. Lastly, the application of magnetic shielding is a small but very important step towards achieving magnetic cleanliness of spacecraft. This effort can be improved by combining it with other methods such as layout optimization and in-orbit magnetic dipole compensation.

In conclusion, this study underscores the potential of a simple Mu-metal shield in addressing both static and dynamic magnetic interference issues from the wheel motor. This opens the door for further research and multidisciplinary strategies to ensure the overall effectiveness of spacecraft systems in managing magnetic cleanliness.

## REFERENCES

- [1] R. Triharjanto, W. Hasbi, A. Widipaminto, et al., Lapan-Tubsat : micro-satellite platform for surveillance & remote sensing, In: Warmbein B (ed) *Proceedings of The 4S Symposium: Small Satellites, Systems and Services (ESA SP-571)*, La Rochelle, France: CDRON., id.35.1, 2004, pp. 20–24.
- [2] S. Hardhienata, R. H. Triharjanto, M. Mukhayadi, LAPAN-A2 : Indonesian Near-Equatorial Surveillance Satellite, *Present 18th Asia-Pacific Reg Sp Agency Forum (APRSAF), Singapore*.
- [3] W. Hasbi, Suhermanto, Development of LAPAN-A3 / IPB Satellite an Experimental Remote Sensing Microsatellite, *34th Asian Conf Remote Sens 2013, ACRS 2013* 2013; 8.
- [4] M. Mukhayadi, R. Madina, U. Renner, Attitude control of bias momentum micro satellite using magnetic and gravity gradient torque, *Proceeding - ICARES 2014 2014 IEEE Int Conf Aerosp Electron Remote Sens Technol* 2014; 132–136.
- [5] M. A. Saifudin, M. Mukhayadi, Attitude Determination and Control System (ADCS) of LAPAN-A2/Orari Satellite, *Media Dirgantara*, 2015, pp. 39–46.
- [6] S. Utama, M. A. Saifudin, M. Mukhayadi, Momentum Biased Performance of LAPAN-A3 Satellite for Multispectral Pushbroom Imager Operation, *IOP Conf Ser Earth Environ Sci* 2018; **149**: 012062.
- [7] M. Mukhayadi, *Efficient and High Precision Momentum Bias Attitude Control for Small Satellite*, der Technischen Universität Berlin, 2021.
- [8] M. Mukhayadi, M. A. Saifudin, Perancangan dan Pengujian Torquer Magnetik untuk Sistem Kendali Sikap Satelit LAPAN-ORARI/A2, In: *Pengembangan Teknologi Satelit di Indonesia : Sistem, Subsystem, dan Misi Operasi*, Bogor: IPB Press, 2013, pp. 174–184.
- [9] S. Utama, P. R. Hakim, M. Mukhayadi, Quarter orbit maneuver using magnetorquer to maintain spacecraft angular momentum, In: *IOP Conference Series: Earth and Environmental Science*. 2019, Epub ahead of print 2019. DOI: 10.1088/1755-1315/284/1/012046.
- [10] E. Carrubba, A. Junge, F. Marliani, et al., Particle swarm optimization for multiple dipole modeling of space equipment, *IEEE Trans Magn*; 50, Epub ahead of print 2014, DOI: 10.1109/TMAG.2014.2334277.
- [11] X. Chen, S. Liu, T. Sheng, et al., The satellite layout optimization design approach for minimizing the residual magnetic flux density of micro- and nano-satellites, *Acta Astronaut* 2019, **163**: 299–306.
- [12] C. Jéger, *Determination and compensation of magnetic dipole moment in application for a scientific nanosatellite mission*, KTH Royal Institute of Technology, 2017.
- [13] A. Lassakeur, C. Underwood, Magnetic cleanliness program on cubesats for improved attitude stability, *Proc 9th Int Conf Recent Adv Sp Technol RAST 2019* 2019, **13**: 123–129.
- [14] T. Inamori, N. Sako, S. Nakasuka, Magnetic dipole moment estimation and compensation for an accurate attitude control in nano-satellite missions, *Acta Astronaut* 2011, **68**: 2038–2046.
- [15] A. Annenkova, N. Abdelrahman, D. Ivanov, et al., CubeSat magnetic atlas and in-orbit compensation of residual magnetic dipole, *Proc Int Astronaut Congr IAC*, 2020-Octob.
- [16] A. Nicolai, S. Stoltz, O. Hillenmaier, et al., Towards a Magnetically Clean Reaction Wheel with Active Magnetic Field Mitigation, *Proc 2019 ESA Work Aerosp EMC, Aerosp EMC 2019*, 1. Epub ahead of print 2019, DOI: 10.23919/AeroEMC.2019.8788947.
- [17] D. A. Nicolai, *Magnetic Field Mitigation Strategies towards a Magnetically Clean Reaction Wheel vorgelegt von zur Erlangung des akademischen Grades genehmigte Dissertation Promotionsausschuss*.
- [18] C. T. Judianto, Utilization of LAPAN-TUBSAT Surveillance Satellite for Natural Disaster Monitoring, In: *Proc 34th Asian Conference on Remote Sensing*, 2013.
- [19] M. A. Saifudin, A. Karim, Mujtahid, LAPAN-A4 Concept and Design for Earth Observation and Maritime Monitoring Missions, *ICARES 2018 - Proc 2018 IEEE Int Conf Aerosp Electron Remote Sens Technol* 2018, **5**: 44–48.
- [20] K. Dang, P. Narvaez, J. Berman, et al., Magnetic Shielding Concepts for Reaction Wheel Assembly on NASA Europa Clipper Spacecraft, *2020 IEEE Int Symp Electromagn Compat Signal/Power Integrity, EMCSI 2020*, 2020, 305–311.